University of Tehran Press

Online ISSN: 2345-475X

DESERT

Home page: https://jdesert.ut.ac.ir/

Forecasting NDVI Variability Using SPI-Driven Hybrid Deep Learning in a Semi-Arid Environment

Saeed Erfani[1*]

[1] Faculty of Natural Resources, Semnan University, Semnan, Iran. E-mail: saeederfani@semnan.ac.ir

Article Info.

Article type:
Research Article

Article history:
Received: 24 Sep. 2025
Received in revised from: 02 Dec. 2025
Accepted: 11 Dec. 2025
Published online: 27 Dec. 2025

Keywords:
CNN-LSTM,
SHAP,
LIME,
Drought Forecasting,
Dryland Agriculture.

ABSTRACT

Effective land management in semi-arid regions is contingent upon the accurate forecasting of vegetative alterations in response to climatic variations. This research utilizes the CNN-LSTM model as a hybrid deep learning framework to predict fluctuations in Normalized Difference Vegetation Index (NDVI) using lagged Standardized Precipitation Index (SPI) and NDVI inputs. The objective of the model is to capture the enduring memory effects of vegetation that impact plant growth, as well as to account for short-term variations in precipitation. A dataset comprising MODIS NDVI and monthly SPI data from 2001–2022 was developed for the region of Semnan, Iran, which is characterized by its extreme aridity. After extensive preprocessing, various configurations of NDVI and SPI lags were systematically assessed. The optimal performance was obtained utilizing one-month SPI values with both 1- and 2-month time lags, in conjunction with a 1-month NDVI lag, resulting in notable accuracy (RMSE = 0.0038; r = 0.968). The application of explainable artificial intelligence methodologies—including SHAP, LIME, and Random Forest feature importance—validated that NDVI lag-1 consistently emerged as the most significant predictor across all analytical approaches. Additionally, SPI lags made substantial contributions, with SPI-1 generally demonstrating a more pronounced impact than lags associated with longer precipitation durations. These results underscore the pivotal influence of short-term vegetative memory and recent precipitation anomalies in determining the dynamics of NDVI within dryland ecosystems.

Cite this article: Erfani, S. (2025). Forecasting NDVI Variability Using SPI-Driven Hybrid Deep Learning in a Semi-Arid Environment. DESERT, 30 (2), DOI: 10.22059/jdesert.2025.105496

DOI: 10.22059/jdesert.2025.105496

Publisher: University of Tehran Press

1. Introduction

Vegetation is a fundamental component of the Earth's ecological systems, playing a central role in regulating biogeochemical cycles, stabilizing climate processes, and supporting essential ecosystem services such as soil protection, water-cycle regulation, and food production (Chapin *et al*., 2000; Bonan, 2008). In semi-arid environments, vegetation dynamics are highly sensitive to fluctuations in precipitation and temperature, making an understanding of climate–vegetation interactions crucial for sustainable land and water management. Monitoring vegetation change at landscape scales increasingly relies on satellite-based indicators, particularly the Normalized Difference Vegetation Index (NDVI), which has become one of the most widely used proxies of vegetation greenness since its introduction by Tucker (1979). Derived from red and near-infrared reflectance, NDVI provides valuable information on plant vigor, phenology, and stress responses (Glenn *et al*., 2008; Hiep *et al*., 2023). The long-term consistency and high temporal resolution of MODIS observations (Justice *et al*., 1998; Huete *et al*., 2002) have greatly expanded the ability of researchers to characterize vegetation dynamics across diverse ecosystems, including dryland regions.

Among climatic drivers, precipitation variability is a key factor shaping vegetation behavior, particularly in water-limited regions. The Standardized Precipitation Index (SPI) (McKee *et al*., 1993) is widely used to quantify meteorological drought at multiple timescales and has proven effective in capturing both short-term soil moisture deficits and longer-term hydrological anomalies that influence vegetation responses. Extensions such as the SPEI incorporate evaporative demand and further enhance drought characterization (Vicente-Serrano *et al*., 2010). Numerous studies have documented that vegetation commonly responds to precipitation anomalies with temporal lags—reflecting delays in soil moisture recharge, root-zone water uptake, and canopy greenness development (Ji & Peters, 2003; Vicente-Serrano *et al*., 2010; Wu *et al*., 2015). This lagged behavior highlights the complexity of climate–vegetation interactions and underscores the need for analytical tools capable of representing non-linear and time-dependent relationships.

Traditional statistical approaches have been widely used to examine the relationship between climatic variables and vegetation indices; however, such methods often struggle to capture the spatial non-stationarity, temporal dependencies, and nonlinearities inherent in ecological systems (Zhu *et al*., 2017). Consequently, deep learning (DL) and machine learning (ML) approaches have gained prominence in ecological modeling. Architectures such as Convolutional Neural Networks (CNNs) and Long Short-Term Memory (LSTM) networks are particularly well suited to vegetation forecasting because they can extract spatial patterns and model long-term temporal dependencies (Reichstein *et al*., 2019; Muruganantham *et al*., 2022). Recent studies have demonstrated the superiority of DL-based models for predicting vegetation indices, drought conditions, and other biophysical parameters, often outperforming traditional regression techniques (Wu *et al*., 2019; Chen *et al*., 2021; Sun *et al*., 2023; Xiao *et al*., 2024). Parallel advances in explainable artificial intelligence (XAI) have further enabled researchers to interpret the internal behavior of complex models, offering insights into variable importance and the interactions that shape ecological outcomes (Zingaro *et al*., 2024).

It is important to note that the present study focuses on forecasting vegetation dynamics indirectly through NDVI, a satellite-derived indicator of greenness rather than an in-situ ecological measurement of biomass, productivity, or species composition. Although ground-based measurements can provide valuable ecological insight, long-term satellite archives such as MODIS NDVI (2001–2022) remain essential for modeling large-scale vegetation responses

in semi-arid environments. Thus, this study aims to predict NDVI variability as a remote-sensing–based descriptor of vegetation behavior rather than ecological change in the strict biological sense.

Despite substantial methodological advances, several challenges remain in the literature. First, the role of lagged SPI and NDVI signals—key determinants of vegetation memory—is often examined in isolation or without systematic evaluation across multiple lag structures. Second, while hybrid DL models have shown promising performance, their interpretability remains limited, hindering their use in environmental decision-making. Third, few studies have integrated DL with XAI techniques to simultaneously achieve high predictive accuracy and transparent understanding of the climatic drivers of vegetation patterns, particularly in semi-arid regions such as Iran where drought vulnerability is high.

Responding to these gaps, the present study develops and evaluates a hybrid CNN–LSTM model to forecast monthly NDVI in the semi-arid Semnan region of Iran using long-term SPI and MODIS NDVI records (2001–2022). The study specifically (i) systematically analyzes lagged SPI and NDVI configurations to quantify vegetation memory effects and (ii) integrates model predictions with XAI approaches—including Random Forest feature importance, SHAP, and LIME—to enhance interpretability of vegetation–climate relationships. Improving NDVI forecasting in water-limited environments directly supports regional drought monitoring and provides useful insights for agricultural planning and climate adaptation strategies.

2. Materials and methods

2.1 Study Area

Semnan County, located in Semnan Province in north-central Iran (34.89°N, 53.97°E), lies within a predominantly semi-arid climatic zone at an average elevation of approximately 1130 m above sea level. It is bordered by Damghan to the east, Mahdishahr to the north, and Garmsar to the west, forming a transition zone between the Alborz highlands and the central Iranian plateau. The region experiences low annual precipitation of nearly 140 mm, an average annual temperature of about 17 °C, and around 48 frost days per year, reflecting the strong seasonal temperature contrasts typical of dryland environments.

Land cover in Semnan County is dominated by arid and semi-arid rangelands with sparse vegetation, making the area highly sensitive to variations in rainfall and temperature. These characteristics, together with the region's ecological fragility and dependence on precipitation-driven vegetation growth, make Semnan a representative case study for examining climate–vegetation interactions in water-limited ecosystems.

Figure 1 illustrates the spatial boundaries and geographical location of the study area, providing a clear contextual understanding of the region's environmental setting.

2.2 Data Collection

Monthly precipitation data were obtained from the Climate Hazards Group InfraRed Precipitation with Stations (CHIRPS) dataset, a high-resolution product widely used in climate-impact assessments and drought monitoring applications. Following the standard procedure introduced by McKee *et al*. (1993), the CHIRPS monthly precipitation series for 2001–2022 was used to compute the one-month Standardized Precipitation Index (SPI-1). The computation involved fitting a two-parameter gamma distribution to the long-term precipitation record, converting cumulative probabilities to a standard normal variate, and generating a temporally consistent series of precipitation anomalies.

To ensure temporal compatibility with the monthly SPI-1 series, NDVI data were derived from the 8-day MODIS Terra MOD09Q1 v6.1 product (250-m resolution). After applying the product's native cloud and snow masking, 8-day NDVI layers were composited into monthly values. All pixels located outside the administrative boundary of Semnan County were removed prior to spatial aggregation. These steps produced a harmonized monthly time series of precipitation (SPI-1) and vegetation greenness (NDVI) suitable for lagged-relationship analysis and hybrid model development.

A series of preprocessing steps was applied to ensure data quality before model development. First, all variables were normalized using Min–Max scaling to the range [–1, 1], which enhances comparability across heterogeneous time-series inputs and stabilizes model training:

$$\tilde{X} = \frac{X - X_{min}}{X_{max} - X_{min}} \times 2 - 1 \quad (1)$$

Where X is the original value, X_{min} and X_{max} are the minimum and maximum of the series, and $\tilde{X}$ is normalized value of the data in [1, -1].

Outliers were treated using the Interquartile Range (IQR) criterion. Values outside the interval $[Q1-1.5\times IQR, Q3+1.5\times IQR]$, were winsorized to the nearest boundary rather than removed. This strategy maintains temporal continuity, which is essential for lag-based modeling.

Missing monthly values (less than 2% of all observations) were handled using linear interpolation over time, thus preventing disruptions in constructing lagged feature sequences and ensuring the integrity of the input time series.

2.3 Temporal lag design and selection

Lagged values of the Standardized Precipitation Index (SPI) and the Normalized Difference Vegetation Index (NDVI) were evaluated as potential predictors of monthly NDVI, following evidence that vegetation responses to rainfall anomalies commonly exhibit temporal delays (Ji & Peters, 2003; Vicente-Serrano *et al*., 2010; Wu *et al*., 2015). The search space for lag combinations was structured using a three-stage procedure.

Stage 1: Individual SPI lags from 1 to 12 months were examined to capture short-term to annual memory effects.

Stage 2: Sets of SPI lags ({1}, {1,2}, {1,2,3}, {1,6}, {1,3,6}, {1,3,6,9}, {1,3,6,9,12}) were evaluated across forecast horizons $h \in \{1,3,6,12\}$ months.

Stage 3: Each SPI configuration was extended by incorporating NDVI lags L ∈ {1, …,6}.

Lag selection was performed using an expanding-window walk-forward validation procedure to prevent temporal leakage, consistent with established time-series forecasting practice (Hyndman & Athanasopoulos, 2018). For each candidate configuration, model performance was assessed using RMSE and Pearson's correlation coefficient averaged across validation folds, and the configuration yielding the lowest RMSE was retained. The optimal structure for h=1 consisted of $SPI_{1,2}$ combined with $NDVI_1$, which aligns with documented short vegetation memory and sensitivity to recent precipitation anomalies. Final evaluation was conducted on a held-out test segment comprising the last 20% of the time series.

All features at time t exclusively used information available up to t, and normalization parameters were derived from the training set and applied consistently to validation and test subsets, following best practices in ecological deep-learning modeling (Reichstein *et al*., 2019).

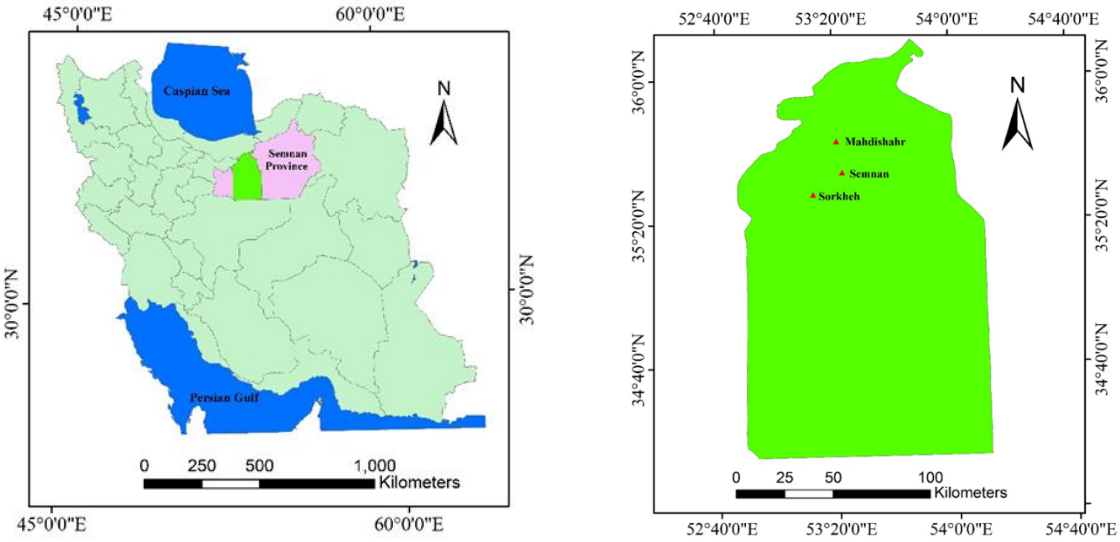

Fig. 1. Semnan Province within Iran; Semnan County and the study area used for NDVI–SPI analysis. Data sources: GADM (countries and subnational boundaries), CHIRPS (precipitation), MODIS (NDVI). Projection: WGS84 (EPSG: 4326);

2.4 CNN-LSTM Hybrid Architecture and Training

To jointly capture short-term temporal patterns and longer-range dependencies, a hybrid 1D-CNN → LSTM architecture was employed. For each month t, the input consisted of a fixed-length vector of lagged predictors [SPI_{t-1}, SPI_{t-2}, …; $NDVI_{t-1}$, …], while the model predicted $NDVI_{t+h}$. The overall framework of the model is illustrated in Figure 2, which outlines the main computational components and their interactions.

Convolutional extraction of local patterns: The lagged sequences were reshaped to (T,F) (time steps × features). A causal Conv1D layer (32 filters, kernel size = 3), followed by MaxPooling1D (pool size = 2), was used to learn short-range temporal motifs, consistent with recommended CNN configurations for time-series feature extraction (LeCun *et al*., 2015).

Sequence modeling: A single LSTM (64 units) layer was used to capture temporal memory and cross-lag dependencies, reflecting the well-established capability of LSTM networks to model nonlinear and delayed ecological responses (Hochreiter & Schmidhuber, 1997; Reichstein *et al*., 2019).

Regularization and output: The regression head consisted of a Dense (32) layer and a linear output neuron. Dropout (0.2) and ReLU activation were applied for regularization. The model was trained using Adam (learning rate 10^{-3}), MSE loss, batch size 16, for up to 100 epochs with EarlyStopping and ReduceLROnPlateau.

Data splitting and leakage control: Hyperparameter/lags were selected using walk-forward validation on the training set. A chronological 80:20 train–test split was used. Standardization parameters were derived exclusively from the training subset, and all sequences were constructed to ensure that month t does not use information from future periods.

This hybrid architecture enables the CNN component to extract short-term temporal patterns from the lagged precipitation inputs (e.g., SPI_{t-1} and SPI_{t-2}), while the LSTM component captures longer-range dependencies by integrating these signals with vegetation memory indicators (e.g., $NDVI_{t-1}$). Together, these layers jointly learn how recent precipitation anomalies and past vegetation conditions contribute to monthly NDVI variability.

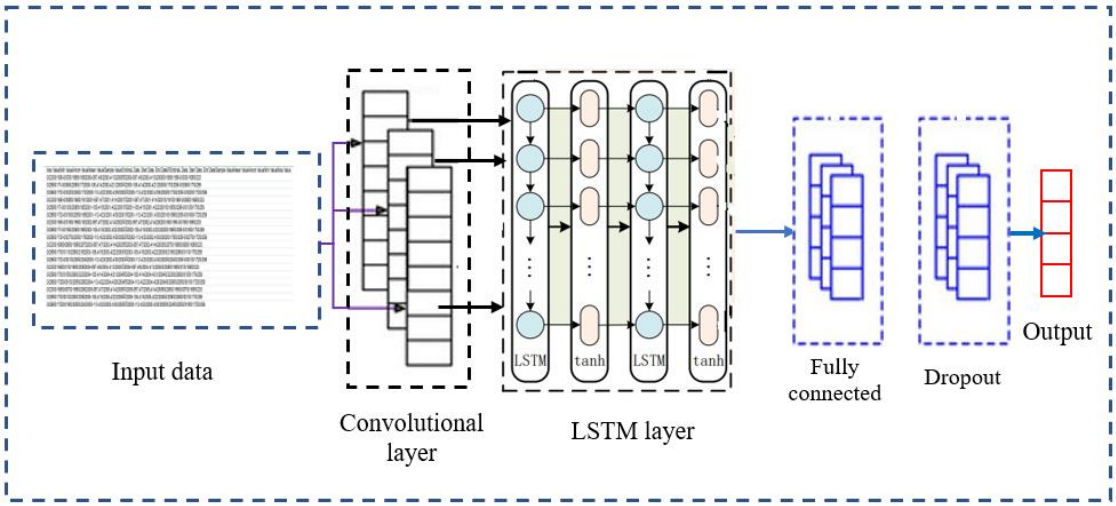

Fig. 2. The CNN-LSTM architecture

2.5 Feature Importance Analysis

In order to drastically enhance the interpretability of the predictive model under consideration, a comprehensive application of diverse methodologies, i.e., Random Forest, SHAP, and LIME, was executed with commitment:

Random Forest was employed as an ensemble-based baseline model to quantify the relative importance of the input features. Random Forest ranks predictors according to their contribution to reducing prediction error, commonly evaluated through the Mean Squared Error (MSE) (Breiman, 2001):

$$MSE = \frac{1}{N}\sum_{i=1}^{N}(y_i - \hat{y_i})^2 \quad (2)$$

Where N is the number of samples, y_i is the actual value in the i-th sample, $\hat{y_i}$ is the predicted value by the model for the i-th sample.

A Random Forest regressor (n_estimators = 500, max_features = 'sqrt', a fixed random state for reproducibility) was trained using the complete predictor set. Feature importance was quantified using impurity-based importance, also known as Mean Decrease in Impurity (MDI), which aggregates each feature's contribution to reducing out-of-bag MSE:

$$MDI\ (X_i) = \sum_{t\in T} p(t).\Delta MSE(t, X_i) \quad (3)$$

Where X_i denotes the feature being evaluated, T is the set of all splitting nodes in a decision tree, $p(t)$ is the probability of reaching node t, and $\Delta MSE(t, X_i)$ represents the reduction in impurity at node t when the split is made on X_i.

A higher MDI score indicates a more influential feature, as such predictors contribute more substantially to impurity reduction across the ensemble of decision trees (Breiman, 2001).

To quantify the contribution of each predictor to NDVI forecasting, SHapley Additive exPlanations (SHAP) were employed. SHAP provides a unified, game-theoretic framework that assigns additive importance values to individual features based on their marginal contributions to the model output (Lundberg *et al*., 2020). In this study, SHAP summary plots and dependence plots were used to visualize how lagged SPI and NDVI inputs influence the predicted NDVI values, allowing clear interpretation of both main effects and feature interactions. These visual

diagnostics facilitate a transparent assessment of the relative influence of short-term precipitation anomalies and vegetation memory on model predictions.

$$\phi_i = \sum_{S \subseteq \{1,\ldots,N\} \setminus \{i\}} \frac{|S|!(|N|-|S|-1)!}{|N|!} (f(S \cup \{i\}) - f(S)) \quad (4)$$

Where ϕ_i is SHAP value for feature X_i, S is a subset of the entire set of features of N without considering i, $f(S)$ is the model prediction value using subset S, $|S|$ is the number of elements in the subset S, $|N|$ is the total number of features.

To provide localized interpretability for individual NDVI predictions, the LIME-Tabular method was applied to selected test-month instances using a sample size of 5000, default kernel width, and discretization enabled for continuous variables. LIME constructs a sparse linear surrogate model g(z) in the neighborhood of each instance, producing signed feature weights that indicate the direction and magnitude of each predictor's local influence. All LIME analyses were conducted exclusively on the out-of-sample test set to ensure that the resulting explanations reflect generalizable model behavior rather than artifacts of the training data (Ribeiro *et al*., 2016).

2.6 Model Evaluation Metrics

To ensure a comprehensive and interpretable assessment of the model's predictive skill and reliability, the performance of the proposed CNN–LSTM hybrid architecture was evaluated using widely adopted statistical metrics and graphical diagnostics. These evaluation procedures are standard in time-series forecasting and machine-learning validation frameworks, providing quantitative and visual insights into model accuracy, bias, and temporal consistency (Willmott & Matsuura, 2005).

2.6.1 Root Mean Squared Error (RMSE)

The RMSE quantifies the average magnitude of prediction errors and is expressed in the same units as the target variable (here, NDVI). RMSE penalizes larger deviations more heavily and is widely regarded as one of the most interpretable accuracy metrics in environmental and geophysical modeling (Willmott *et al*., 2005):

$$RMSE = \sqrt{\frac{1}{N}\sum_{i=1}^{N}(y_i - \hat{y}_i)^2} \quad (5)$$

where y_i is the observed NDVI at sample i, $\hat{y}_i$ is the model prediction, and N is the number of observations. Lower RMSE values indicate greater predictive accuracy.

2.6.2 Pearson correlation coefficient (r)

Pearson's correlation coefficient r measures the strength of the linear association between observed and predicted NDVI values. It helps assess the extent to which the model captures temporal variability and directionality in vegetation dynamics (Willmott *et al*., 2005):

$$r = \frac{\sum(y_i - \bar{y})(\hat{y}_i - \bar{\hat{y}})}{\sqrt{\sum(y_i - \bar{y})^2 \sum(\hat{y}_i - \bar{\hat{y}})^2}} \quad (6)$$

Where $\bar{y}$ and $\bar{\hat{y}}$ denote the sample means of observed and predicted values, respectively. Values of r close to 1 (or −1) indicate strong positive (or negative) linear agreement.

2.6.3 Coefficient of determination (R^2)

The R^2 expresses the proportion of variance in observed NDVI that is explained by the predictive model. It complements RMSE and r by indicating how well the model reproduces overall variability (Willmott *et al*., 2005):

$$R^2 = 1 - \frac{\sum(y_i - \hat{y}_i)^2}{\sum(y_i - \bar{y})^2} \quad (7)$$

2.6.4 Graphical diagnostics.

Graphical diagnostics (e.g., observed–predicted scatter plots, residual patterns, and correlation heatmaps) were used to visually assess model bias, heteroscedasticity, and temporal consistency, following standard recommendations for time-series model evaluation (Hyndman & Athanasopoulos, 2018).

2.7 Interpretability Assessment

To quantify and interpret the influence of lagged climatic and vegetation predictors on model outputs, model-agnostic interpretability frameworks were employed. Specifically, SHAP (Lundberg *et al*., 2020) and LIME (Ribeiro *et al*., 2016) were applied alongside impurity-based feature importance from a Random Forest regressor (Breiman, 2001). These approaches provide complementary perspectives: SHAP assigns additive contribution scores based on cooperative game theory, LIME fits sparse local surrogate models around individual predictions, and Random Forest importance quantifies reductions in prediction error attributable to each feature.

The interpretability results were visualized using summary plots, dependence plots, and local explanation diagrams, enabling a clear examination of how individual lagged SPI and NDVI inputs shape the predicted NDVI values. In addition, standard diagnostic charts—including scatter plots, residual plots, correlation heatmaps, and prediction-error histograms—were incorporated to contextualize interpretability outputs within the model's overall error structure (Willmott, 2005).

Together, these interpretability procedures offer a transparent assessment of model behavior and ensure that the hybrid CNN–LSTM framework remains both robust and explainable when applied to forecasting vegetation dynamics under variable climatic conditions.

3. Results and discussion

3.1. Evaluation of NDVI Prediction Models

3.1.1 Investigating the Effect of Time Lags in the CNN-LSTM Combined Model

As shown in Table 1, the highest predictive performance among SPI-only configurations was achieved when the model used monthly SPI lags of 1, 3, 6, and 9 months prior to the forecast month for a one-month-ahead NDVI prediction.

Although multiple forecast horizons (h = 1, 3, 6, and 12 months) were initially evaluated during model screening, it is noteworthy that the best-performing models across all experiments consistently corresponded to a one-month prediction horizon. Consequently, the subsequent analysis and interpretation focus on short-term (one-month-ahead) forecasting results, as these emerged objectively from the performance ranking rather than from an a priori modeling choice.

To maintain clarity and avoid excessively long tables, only the top 10 lag-set combinations—ranked by RMSE and Pearson's correlation coefficient—are reported in Table 1, while configurations yielding negative correlations were omitted. Each entry represents the best

outcome obtained after 10 independent runs of the hybrid CNN–LSTM model, ensuring robustness against random initialization effects.

Table 1. Top 10 combinations resulting from running the model with different SPI delay

Correlation	RMSE	Forecast Horizon	Lags_5	Lags_4	Lags_3	Lags_2	Lags_1
0/469	0/0129	1		9	6	3	1
0/468	0/0130	6	12	9	6	3	1
0/459	0/0191	1	12	9	6	3	1
0/395	0/0135	3	12	9	6	3	1
0/378	0/0132	3			6	3	1
0/368	0/0138	1			6	3	1
0/345	0/0173	6		9	6	3	1
0/333	0/0165	12	12	9	6	3	1
0/327	0/0136	12			3	2	1
0/324	0/0148	6			3	2	1

To illustrate, if the target month is January, the optimal lag combination implies that $NDVI_{t+1}$ can be most accurately predicted using SPI readings from November, September, June, and March of the preceding year. Even so, the best configuration yields a Pearson correlation coefficient of $r \approx 0.47$ ($R^2 \approx 0.22$), meaning that approximately 20% of the NDVI variance is explained by these lagged precipitation inputs. Although the RMSE value reflects a relatively small average deviation between observed and predicted NDVI values, the moderate explanatory power indicates that precipitation alone—represented through SPI—accounts for only a limited portion of vegetation variability in this semi-arid region.

The scatter plot of observed versus predicted NDVI values for the best-performing lag combination (derived from Table 1) is provided below. Overall, results confirm that model accuracy generally declines when (i) the number of SPI lag inputs is reduced or (ii) lags become increasingly distant from the prediction horizon—both patterns consistent with the short-term memory behavior of vegetation in water-limited ecosystems.

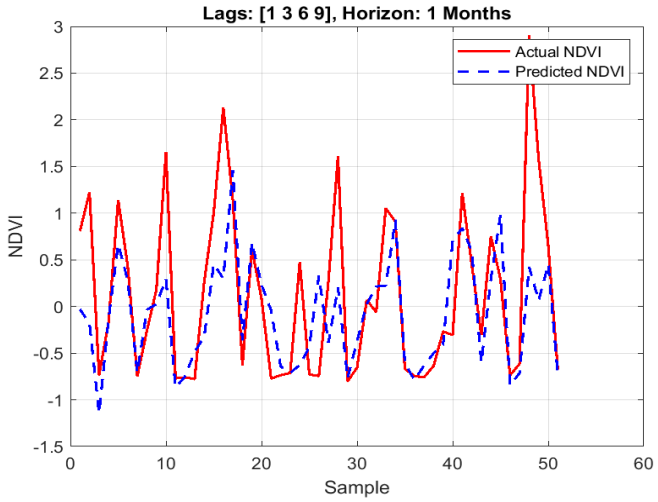

Fig. 3. Predicted value vs. actual value of NDVI with only SPI lag as input variable

3.1.2 Effect of Combining SPI Lags and Adding NDVI Lag

Initial results showed that using a single SPI lag alone limited model accuracy, and the correlation coefficient was low in many combinations. Therefore, combinations of several SPI lags that improved the model were considered. However, the best improvement was achieved when a time lag of NDVI was also added as an input variable. This modification explicitly accounts for vegetation memory and persistence effects, which are well documented in NDVI time series. The results of the top 10 combinations are shown in Table (2).

Table 2. Top 10 combinations resulting from running the model with different combinations of SPI lag and NDVI lag

Correlation	RMSE	NDVI_Lag	Forecast Horizon	Lags_4	Lags_3	Lags_2	Lags_1
0/968	0/0038	1	1			2	1
0/966	0/0045	1	1				1
0/955	0/0051	2	1			6	1
0/925	0/0063	1	2			6	1
0/913	0/0048	1	2				1
0/880	0/0149	2	2			2	1
0/871	0/0067	2	1			2	1
0/870	0/0111	1	1			6	1
0/849	0/0083	2	3			2	1
0/843	0/0074	1	3				1

It is clearly evident that with this modification, higher accuracy predictions can be made with simpler combinations of SPI time lags. For the example mentioned in the previous section, to predict vegetation cover one period (month) ahead, only a combination of the previous 1 and 2 periods' SPI lags, along with the previous period's NDVI lag, is sufficient to estimate vegetation cover with significantly higher accuracy ($R^2 = 0.938$). Furthermore, the correlation coefficient for the best results obtained at each stage improved by more than two-fold, and the RMSE decreased from 0.0128 to 0.0038. This confirms that short-term NDVI persistence dominates predictive skill, while precipitation acts as a secondary but still relevant driver.

Importantly, the high correlation values obtained after adding NDVI lag should be interpreted cautiously. These values primarily reflect the strong temporal autocorrelation inherent in NDVI time series, rather than an exclusive climatic control. Thus, the role of SPI should be viewed as modulating vegetation dynamics rather than fully determining them.

3.1.3 Comparison of the Best Combinations and Prediction Error Analysis

Based on the obtained results, the three best combinations were selected based on the lowest RMSE and highest correlation, and their performance was carefully examined. This section compares the actual NDVI values with the model predictions for these combinations to determine the model's accuracy.

As seen in Figure 4, the predicted values in the model resulting from the combination of 1 and 2-month lags of SPI with a 1-month lag of NDVI accurately follow the actual trajectory of NDVI changes. This correlation is observable even at the peaks and valleys of the trajectory. The next model, which only lacks the 2-month lag of the SPI variable, deviates slightly from the actual values in the valleys. In the third model, where the SPI variable is created from a

combination of 1-month and 6-month lags, there is deviation at some peaks and all valleys. Crucially, referring to Table 2, adding the NDVI variable lag from 2 months to 1 month In the third model, reduces the correlation from 0.95 to 0.87. This could mean that the effects of rainfall 6 months prior can impact vegetation 2 months before the observation time.

Although SPI_6 appears to exert a positive influence in some global analyses (Table 2), its effect is not uniform. In fact, the influence of SPI_6 varies across analytical methods and temporal contexts, reflecting the scale-dependent and non-linear nature of precipitation–vegetation interactions in semi-arid environments. Such behavior is consistent with previous studies reporting delayed or indirect vegetation responses to antecedent rainfall at seasonal to sub-seasonal scales.

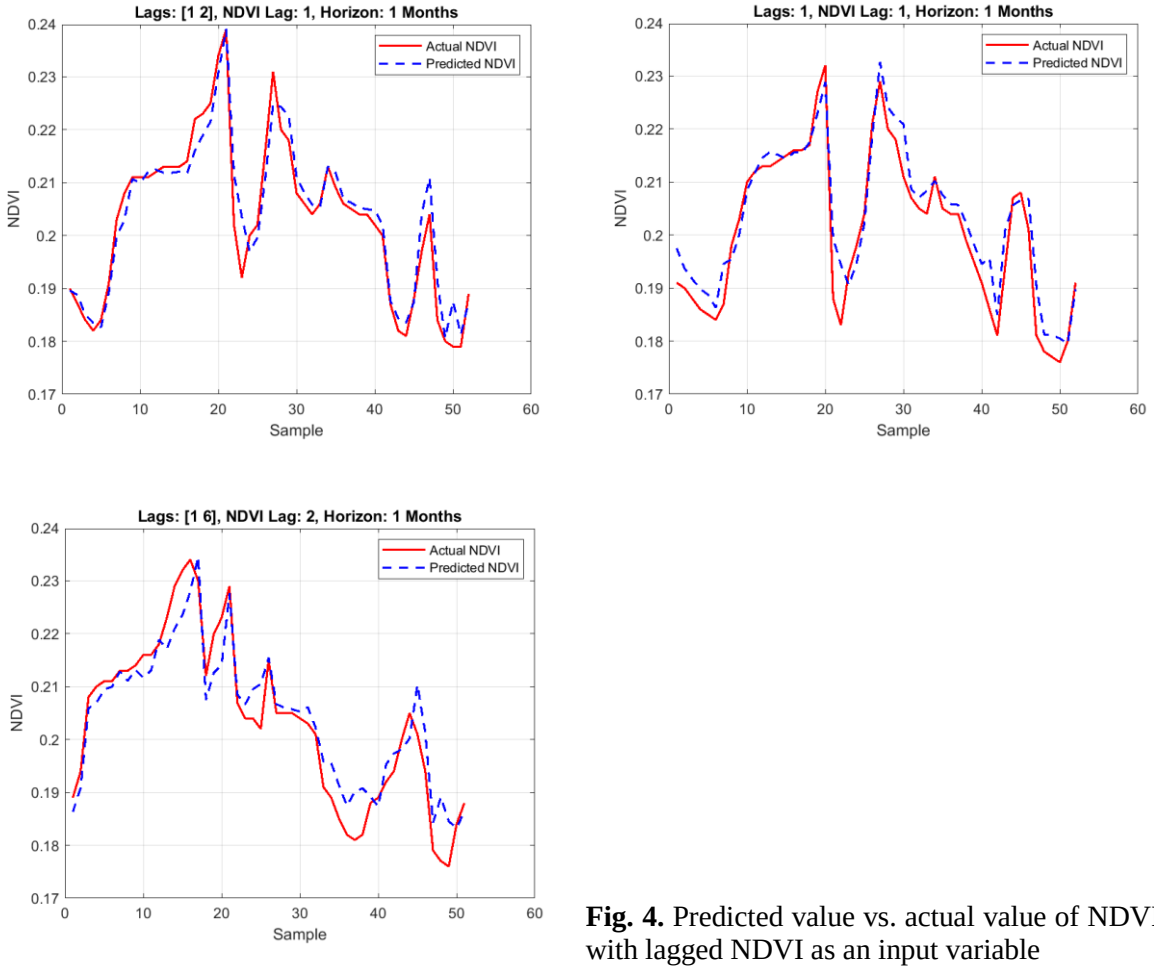

Fig. 4. Predicted value vs. actual value of NDVI with lagged NDVI as an input variable

Even while the hybrid Convolutional Neural Network-Long Short-Term Memory (CNN-LSTM) model has proven a generally acceptable performance in the context of forecasting variations in the NDVI, it's important to note that there have been apparent and significant prediction errors that have appeared during certain temporal segments, usually termed as troughs, wherein NDVI values have dramatically fallen. Many of elements contributing to these disparities in prediction accuracy call for thorough investigation. First, it is vital to realize that sudden and quick declines in NDVI are often related with non-repetitive and unexpected

environmental events including extended drought conditions, changes in land use patterns, outbreaks of pests, or several kinds of human interventions—all of which pose significant obstacles for the model's ability to generalize properly given their rare occurrence and the complicated nature of the underlying processes. Moreover, the current model mostly depends on historical lagged values of SPI and NDVI, which may not fully cover the whole spectrum of causal variables at work throughout these abrupt changes, hence restricting its predictive power. Furthermore, there is the chance of temporal misalignment between the climatic input parameters and the vegetative response; for example, the late reaction of vegetation to total losses in rainfall might further aggravate these predictive errors. At last, one should keep in mind that observational noise found in NDVI measurements, especially during days of overcast weather or during changing seasons, might drastically impede the model's learning process and general accuracy. Given these discovered constraints, it is vital that upcoming research efforts concentrate on combining a wider spectrum of environmental factors and utilize more readable and open deep learning architectures as such developments might possibly improve the model's accuracy and robustness during these important and sensitive phases of NDVI forecasting.

3.2 Feature Analysis

The evaluation process of the CNN-LSTM combined model continued with the application of various feature analysis methods to enhance model transparency and better understand the role of input variables in NDVI prediction. This section comprises three subsections:

3.2.1 Feature Importance Analysis with Random Forest

To assess the impact of each time lag of SPI and NDVI lag on the predicted NDVI value, the Random Forest Regressor algorithm was employed. As a non-parametric tree-based algorithm, this model allows for the calculation of the relative importance of features using metrics such as Mean Squared Error (MSE) reduction and the coefficient of determination (R^2).

Figure 5 shows that in all three combinations, the effect of NDVI lag is significantly higher than the other two variables on the output. The MSE and R^2 values indicate a highly satisfactory accuracy of the Random Forest analysis results for the predicted outputs in all three combinations. For a better visual understanding of the importance of each model feature, a heatmap of the top three combinations is presented in Figure 6.

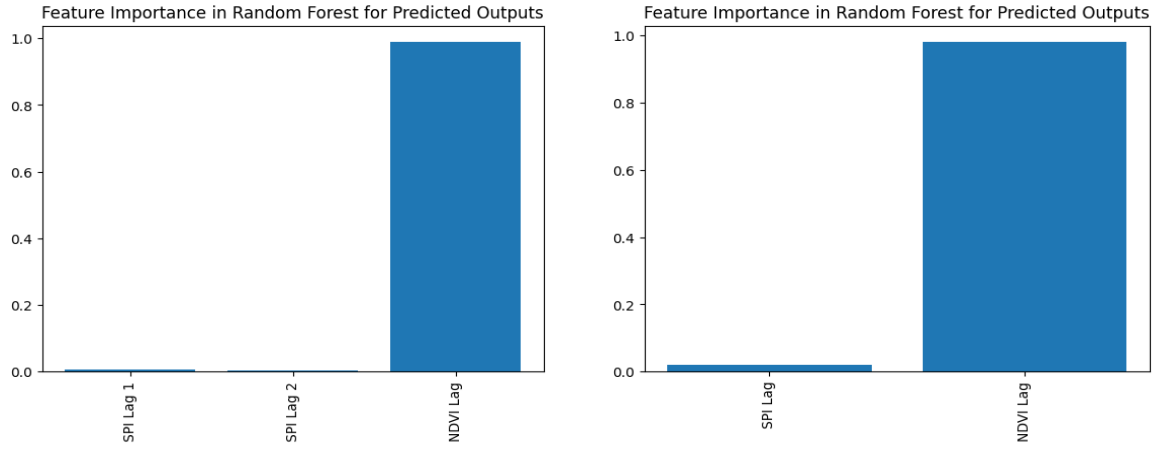

a) SPI Lags [1,2], NDVI Lag [1]. MSE: 12.96e-06, R^2: 0.940 b) SPI Lags [1,0], NDVI Lag [1]. MSE: 19.36e-06, R^2: 0.907

Fig. 5. Relative importance chart of features for the top three combinations

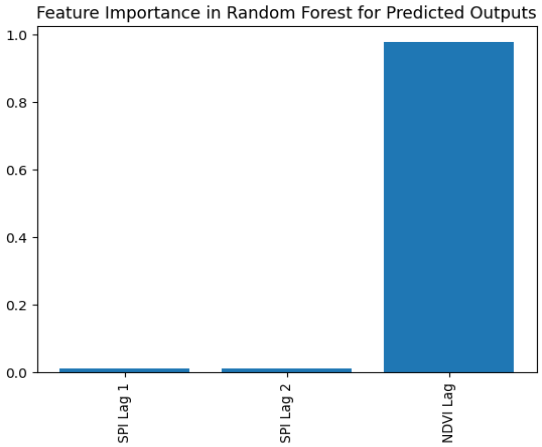

c) SPI Lags [1,6], NDVI Lag [2]. MSE: 24.01e-06, R^2: 0.897

Fig. 5. Continued

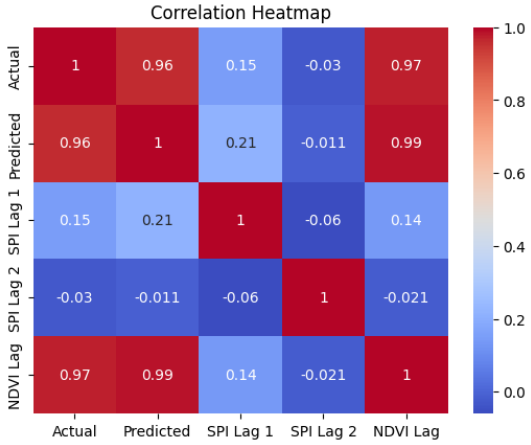

a) SPI Lags [1,2], NDVI Lag [1]

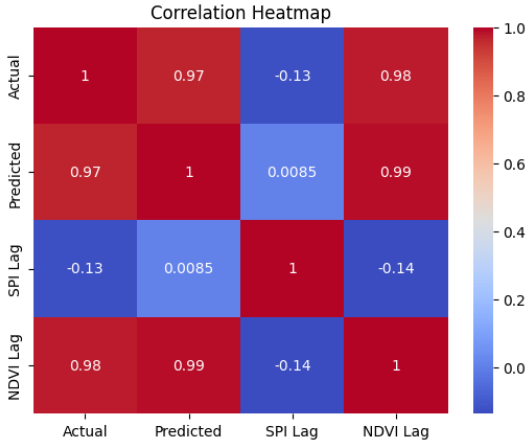

b) SPI Lags [1,0], NDVI Lag [1]

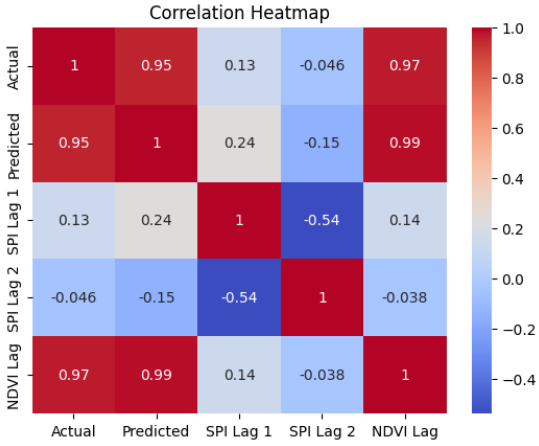

c) SPI Lags [1,6], NDVI Lag [2]

Fig. 6. Heatmap of the relative importance of features for the top three combinations.

As shown in Figure (6a), the correlation between Actual and Predicted NDVI is 0.96. This very high value indicates that the deep learning model has successfully predicted the trend and actual values of NDVI with high accuracy. Such a high value indicates the model's acceptable performance in reproducing the behavior of the target variable.

The correlation between NDVI Lag and Predicted is 0.99, and with Actual is 0.97. This indicates that the previous month's NDVI plays a very important role in predicting the current NDVI. In other words, the NDVI itself in past times (lag=1) has a strong temporal memory in predicting the future, which has also affected the learning model. Therefore, including the lagged NDVI in the model has increased its predictive power.

SPI Lag 1 has a correlation of 0.21 with Predicted and 0.15 with Actual. This shows that SPI one month prior has a weak but noticeable effect on the current NDVI. This is logical, as the effect of rainfall with a short time lag (about one month) can affect vegetation cover.

SPI Lag 2 has almost no correlation (Actual = -0.03) and (Predicted = -0.011). It seems that the effect of rainfall with a two-month lag has no significant role in predicting NDVI for this region or time period.

The results in Figures (6b) and (6c) are similar to the previous combination and show the weak but noticeable effect of rainfall one month prior on the current vegetation. What is observed from the images is that by adding a lag to the precipitation index, the effect of the one-month prior precipitation lag on the Actual and Predicted data improves.

3.2.2 Feature Dependency Analysis with SHAP Values

To interpret the output of the CNN-LSTM model and gain a deeper understanding of how features affect NDVI prediction, the SHAP (SHapley Additive exPlanations) method was used. This tool locally and globally analyzes the impact of each feature on the model's output, helping to better identify non-linear relationships and complex interactions between features.

Figure (7a) shows that NDVI Lag has the highest dispersion and a positive impact on the output. High values (red) lead to an increase in the predicted NDVI value, while low values (blue) have a decreasing effect.

The 2-month lagged rainfall is mostly distributed around a SHAP value of zero, meaning its influence is weaker and closer to neutral. However, the slight dispersion of red/blue points indicates a minor positive and negative impact. Meanwhile, the 1-month lagged rainfall has almost no effect; its SHAP values are very close to zero, and the colors do not show a dispersed distribution.

Figure (7b) also shows the wide distribution of NDVI Lag points relative to the vertical axis, indicating that this feature plays a dominant role in NDVI prediction. Red points (higher NDVI Lag values) are concentrated on the right (positive SHAP values), indicating that high NDVI Lag values lead to an increase in the next month's NDVI prediction, and conversely, low values cause a decrease in the vegetation index prediction. SPI Lag points are distributed around a SHAP value of zero and have a smaller range than NDVI Lag. However, the dispersion pattern suggests that the effect of the previous month's rainfall lag on NDVI prediction is relatively significant, and an increase in this feature value leads to a higher vegetation cover in the following month.

In Figure (7c), NDVI Lag remains the most important predictor for the next month's NDVI; it has a strong positive and negative influence depending on the past NDVI value. This index confirms that the previous month's NDVI is the most important driver of the model in all combinations. SPI Lag1 and SPI Lag2 are both centered near zero, although the effect of the 1-

month rainfall lag is less than the effect of the 6-month rainfall lag on the prediction, but this effect is direct. That is, increased rainfall in the previous month contributed to increased vegetation cover one month later. However, the 6-month rainfall lag shows an inverse effect on vegetation cover one month later. This means that whenever rainfall 6 months prior to the study date was lower, the vegetation covers one month after that date was better (for example, in some periods, high rainfall 6 months prior may reduce vegetation cover due to waterlogging or saturation).

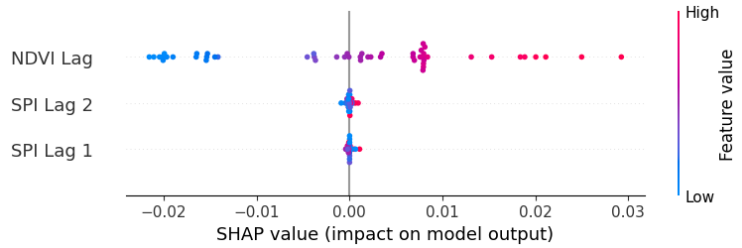

a) SPI Lags [1,2], NDVI Lag [1]

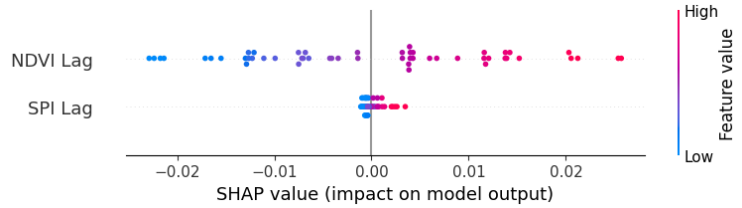

b) SPI Lags [1,0], NDVI Lag [1]

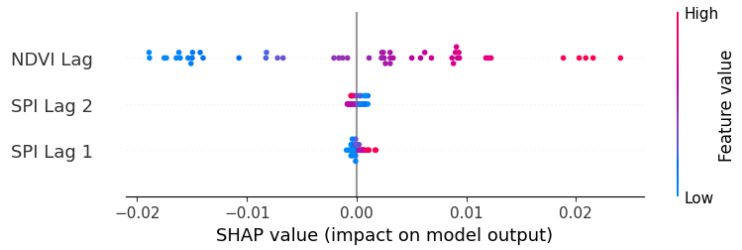

c) SPI Lags [1,6], NDVI Lag [2]

Fig. 7. SHAP Summary chart for the top three combinations.

The charts in Figure (7) generally show that the maximum SHAP value for NDVI Lag in all three combinations reaches approximately +0.025. The SHAP range for SPI Lag1 and Lag2 is very small (approximately ±0.005), indicating their minimal influence.

The charts in Figure (8) show the relationship between the NDVI Lag value and its SHAP value. The color of the points indicates the value of the second feature (SPI Lag).

In Figure (8a), an almost linear positive relationship is observed between the NDVI Lag value and its SHAP value. As NDVI Lag increases, its impact on the model output also increases. The color of the points (representing the SPI Lag2 value) is scattered throughout the chart but does not significantly alter the relationship. This means that the 2-month rainfall lag has little effect on adjusting the role of NDVI Lag. In other words, the effect of NDVI Lag

increases linearly independently of the rainfall index lag value. This analysis also holds true for Figures (8b) and (8c), but the effect of the 1-month rainfall lag on adjusting the role of the vegetation index lag is examined.

In conclusion, NDVI Lag has a direct and strong influence on the output and is not affected by the value of the previous month's rainfall lag.

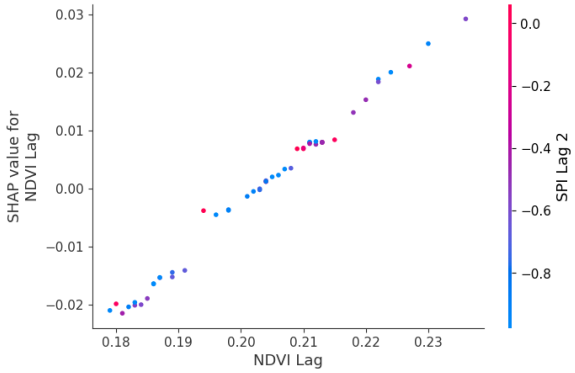

a (SPI Lags [1,2], NDVI Lag [1]

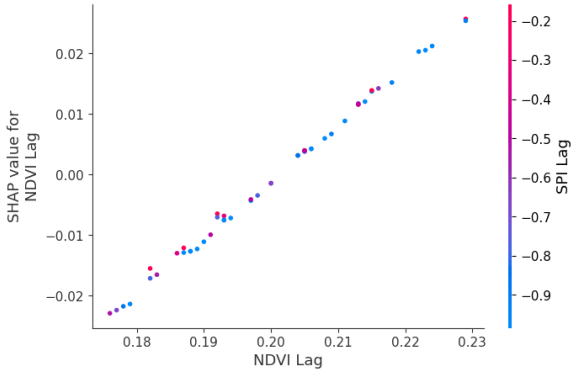

b (SPI Lags [1,0], NDVI Lag [1]

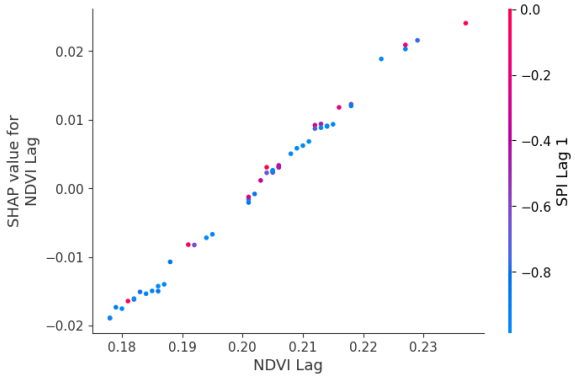

c (SPI Lags [1,6], NDVI Lag [2]

Fig. 8. SHAP Value Dependence Plot for the most important feature in the top three combinations.

In all three combinations, increasing the NDVI Lag value leads to an increase in the SHAP value. This means that, generally, the higher the NDVI in the previous month, the stronger the model's prediction of a higher NDVI in the following month. The color-coding of the points shows that different values of SPI Lag (one or two months depending on the combination) have a minor effect on the main slope of the relationship. In points with cool colors (low SPI values), a slight deviation towards negative SHAP is observed. In points with warm colors (high SPI values), they often shift the SHAP graph towards positive values, but this relative change is very small. This means that rainfall with a one or two-month lag can slightly enhance the effect of NDVI Lag at high values or slightly weaken it at low values, but the main role still returns to the linear and direct relationship with NDVI Lag. NDVI Lag is the basis of the modeling. With an increase in the previous month's NDVI lag, the model expects a higher NDVI in the current month. SPI Lag acts as a minor modifier. Higher SPI values may slightly increase the impact of NDVI Lag (warmer points slightly above the general trend line), while lower SPI values slightly decrease the SHAP at the same NDVI Lag value.

3.2.3 Local Analysis with LIME

To examine and understand the model's behavior in specific instances (local interpretability), the LIME (Local Interpretable Model-agnostic Explanations) algorithm was used. This tool simplifies the main model around a specific point, showing how the features affect the prediction of that specific instance.

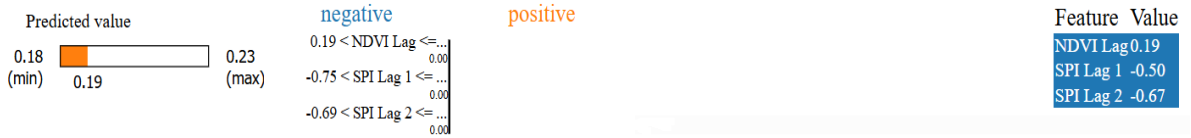

a) SPI Lags [1,2], NDVI Lag [1]

b) SPI Lags [1,0], NDVI Lag [1]

c) SPI Lags [1,6], NDVI Lag [2]

Fig. 9. LIME diagram for the effect of features on the top three combinations.

In Figure (9a), the locally predicted value is approximately 0.19. NDVI Lag has the greatest impact on the prediction. However, NDVI lags greater than 0.19 have a decreasing effect on the predicted value, and the local value of this feature is 0.19, hence it is shown as negative. After NDVI lag, the 1-month previous rainfall lag affects the predicted value. As observed, values greater than -0.75 had a decreasing (negative) effect on the predicted vegetation cover of the following month, and therefore the local value of -0.50 is displayed negatively. The least impact is related to the 2-month previous rainfall lag, where the local value of -0.67, being greater than -0.69, has a decreasing (negative) effect on the predicted value.

In Figure (9b), the locally predicted value is approximately 0.19. NDVI Lag is again the strongest driver of the output value, and its local value is the same as before. SPI Lag 1 (-0.33) is the only rainfall lag with a negative role here because, in this combination, according to the LIME analysis, SPI lag values greater than -0.50 have a decreasing effect on the output NDVI 1 month later.

In Figure (9c), the locally predicted value is approximately 0.19. NDVI Lag, despite being a two-period lag, is still the most effective factor in predicting vegetation cover one month ahead. However, here, NDVI lags smaller than 0.19 showed a decreasing effect on the output variable. Regarding the standardized precipitation index lag, the 6-month lag was more effective than the 1-month lag in predicting vegetation cover. Precipitation values greater than -0.93 for the 6-month SPI lag had a decreasing effect and greater than -0.85 for the 1-month SPI lag had an increasing effect on vegetation cover. It can be said that the local values of SPI Lag 1 (-0.67) have a relatively strong increasing role in the prediction, although the precipitation of the last 6 months is more effective in predicting the vegetation index.

As observed, in all three combinations, NDVI Lag (both one and two periods prior) always has the largest contribution to the prediction of NDVI. This emphasizes that the plant's own vegetation memory (Lagged NDVI) is the main axis of modeling.

Although SPI Lags have a positive effect in most local samples, the magnitude of their effect varies slightly in different combinations.

LIME takes the actual values of the features for each sample and shows their positive/negative impact. This analysis highlights that within different input ranges (e.g., when NDVI Lag equals 0.18 or 0.19), NDVI prediction can be influenced by SPI Lags.

Comparing the three feature analysis tools, Random Forest, SHAP, and LIME, shows that in all of them, the NDVI Lag feature has the highest importance in predicting future NDVI values.

Overall, the analysis showed that the most reliable forecasts were obtained when using SPI lags of one and two months together with an NDVI lag of one month, which achieved the lowest prediction errors (RMSE = 0.0038) and the highest correlation (r = 0.968).

Across all feature analysis methods—Random Forest, SHAP, and LIME—the lagged NDVI variable consistently emerges as the dominant predictor, confirming the central role of vegetation memory. In contrast, SPI lags exhibit weaker and more variable contributions, depending on lag length, season, and local conditions.

Notably, the seemingly inconsistent behavior of SPI_6 across Random Forest, SHAP, and LIME analyses should not be interpreted as a contradiction. Rather, it reflects differences between global importance (RF), average marginal contribution (SHAP), and local instance-specific effects (LIME). This pattern underscores that longer precipitation lags influence NDVI indirectly and episodically, rather than exerting a stable linear effect.

The dominance of lagged NDVI over precipitation-based indices in short-term vegetation prediction observed in this study is consistent with previous findings in arid and semi-arid regions. Numerous studies have demonstrated that vegetation dynamics exhibit strong temporal persistence, reflecting ecosystem memory and delayed physiological responses to climatic forcing. For instance, Weiss *et al*. (2004) showed that NDVI variations in semi-arid ecosystems are strongly influenced by antecedent climatic conditions and that precipitation alone cannot fully explain inter-annual vegetation variability.

Similarly, large-scale analyses have revealed that vegetation anomalies are often driven by antecedent precipitation rather than concurrent rainfall, with time-lag effects extending from one to several months depending on climatic regime and ecosystem type (Papagiannopoulou *et al*., 2017; Wu *et al*., 2015). These lagged responses are frequently associated with soil moisture storage and drought propagation processes, whereby meteorological drought signals propagate into ecological responses over delayed time scales (Huang *et al*., 2017).

In line with these findings, the results of the present CNN–LSTM model indicate that while SPI contributes to NDVI prediction, its explanatory power is secondary to that of lagged NDVI, which encapsulates vegetation memory and integrated ecosystem responses. This outcome supports earlier remote sensing and deep learning studies suggesting that temporal dependencies embedded in vegetation indices often dominate short-term forecasting skill, while climatic variables act primarily as modulators of vegetation dynamics rather than sole predictors (Zhang *et al*., 2016). Overall, the present results reinforce the consensus that short-term NDVI forecasting in water-limited environments is largely governed by vegetation persistence, with precipitation exerting a delayed and indirect influence.

On this basis, the next section turns to the broader ecological meaning of these findings, their practical applications, and the limitations of the proposed CNN-LSTM approach.

4. Conclusion

This research precisely presents an advanced hybrid approach that successfully combines LSTM and CNN architectures, hence incorporating lagged. The main goal of precisely predicting is to use inputs from SPI and NDVI together with advanced explainable AI techniques. The complex interactions of vegetation in Iran's semi-arid Semnan region. This study differs greatly from earlier academic work in that its originality is mainly based on a thorough analysis of several lag. Configurations that elegantly combine short-term rainfall variations with the natural memory effects of plants, while also incorporating interpretable features like Random Forest, SHAP By going beyond the restrictions usually linked to opaque black-box deep learning models and LIME address their limits.

When taken together, the findings of this exhaustive study quite clearly showed that the particular setup using SPI lags of one month and two months was superior. With an NDVI lag of one month, the Root Mean Square indicated the highest level of predictive ability obtained. RMSE error is 0.0038 and the correlation coefficient (r) is 0.968. These major results support the idea that while the lagged NDVI acts as a important measure that accurately reflects the underlying memory and resilience traits found in plant systems. From an ecological perspective, this supports the general knowledge that vegetation responses inside arid and semi-arid areas are distinguished by delays as well as nonlinear dynamics. which are exquisitely formed by the total interaction of soil moisture availability and rainfall patterns.

SHAP and LIME approaches offer a solid framework for interpretability since they regularly find the lagged NDVI as the main predictor while also explaining SPI's role in predictive modeling is context-dependent. For agricultural consultants and legislators charged with the crucial responsibility of creating efficient early warning systems for, such openness is absolutely vital. drought conditions; designing irrigation scheduling techniques; and creating climate adaptation strategies precisely suited for the particular local settings in which they run.

Still, it should be noted that this research was only ever confined to one case study using MODIS data with Moderate Resolution Imaging Spectroradiometer. moderate spatial resolution with fairly limited range of climatic drivers accompanying. Future studies should therefore seek to broaden this analytical framework across a variety of ecosystems, include higher-resolution remote sensing data sources such as Further confirm and improve the robustness of the suggested model, Sentinel-2 and Landsat, and compare the results with those of conventional statistical approaches.

Finally, this study demonstrates that integrating explainable artificial intelligence techniques with deep learning models, specifically the CNN–LSTM framework, can enhance both predictive performance and interpretability in NDVI forecasting. Beyond improving short-term prediction accuracy, the proposed approach provides scientifically interpretable insights into the relative roles of vegetation memory and precipitation variability. These insights contribute to a better understanding of vegetation–climate interactions in semi-arid regions and may support more informed decision-making in land-use management, drought monitoring, and agricultural planning under increasing climate variability and uncertainty.

Author Contributions

S.E. contributed to all aspects of the study, including conceptualization, methodology, software development, validation, formal analysis, investigation, data curation, visualization, manuscript preparation, review and editing, supervision, project administration, and funding acquisition. The author has read and approved the final version of the manuscript.

Acknowledgements
The author would like to thank Dr. Behrooz Arastoo for kindly providing access to the initial NDVI and SPI datasets used in this study. All subsequent data processing, modeling, analysis, and manuscript preparation were conducted independently by the author.

Ethical considerations
This study used publicly available remote sensing and climatic datasets and did not involve human participants or animal subjects. Therefore, ethical approval was not required.

Conflict of interest
The author declares no conflict of interest.

Data Availability Statement
The datasets analyzed in this study were obtained from authorized sources. Due to institutional data use policies, the raw data are not publicly available but may be accessible upon reasonable request and with permission from the original data provider.

Funding
This research did not receive any specific grant from funding agencies in the public, commercial, or not-for-profit sectors.

References

Bonan, G. B. (2008). Forests and climate change: Forcings, feedbacks, and the climate benefits of forests. *Science*, *320*(5882), 1444–1449.

Breiman, L. (2001). Random forests. *Machine Learning*, *45*(1), 5–32. https://doi.org/10.1023/A:1010933404324

Chapin, F. S., Zavaleta, E. S., Eviner, V. T., *et al*. (2000). Consequences of changing biodiversity. *Nature*, *405*(6783), 234–242.

Chen, Z., Liu, H., Xu, C., Wu, X., Liang, B., Cao, J., & Chen, D. (2021). Modeling vegetation greenness and its climate sensitivity with deep-learning technology. *Ecology and Evolution, 11*,7335–7345.

Glenn, E. P., Huete, A. R., Nagler, P. L., & Nelson, S. G. (2008). Relationship Between Remotely-sensed Vegetation Indices, Canopy Attributes and Plant Physiological Processes: What Vegetation Indices Can and Cannot Tell Us About the Landscape. *Sensors*, *8*(4), 2136-2160

Hiep, N.V.; Thao, N.T.T.; Viet, L.V.; Luc, H.C.; Ba, L.H. (2023). Affecting of Nature and Human Activities on the Trend of Vegetation Health Indices in Dak Nong Province, Vietnam. *Sustainability*, *15*, 5695. https://doi.org/10.3390/su15075695

Hochreiter, S., & Schmidhuber, J. (1997). Long short-term memory. *Neural Computation*, *9*(8), 1735–1780. doi: 10.1162/neco.1997.9.8.1735.

Huang, S., Li, P., Huang, Q., Leng, G., Hou, B., & Ma, L. (2017). The propagation from meteorological to hydrological drought and its potential influence factors. *Journal of Hydrology, 547,* 184–195. https://doi.org/10.1016/j.jhydrol.2017.01.041

Huete, A., Didan, K., Miura, T., Rodriguez, E. P., Gao, X., & Ferreira, L. G. (2002). Overview of the radiometric and biophysical performance of the MODIS vegetation indices. *Remote Sensing of Environment, 83*(1–2), 195–213.

Hyndman, R. J., & Athanasopoulos, G. (2018). *Forecasting: Principles and Practice*. (2nd ed.) OTexts. https://otexts.org/fpp2/

Janetzky, P., Gallusser, F., Hentschel, S., Hotho, A., & Krause, A. (2024). Global Vegetation Modeling with Pre-Trained Weather Transformers. *arXiv (Cornell University),* https://doi.org/10.48550/arxiv.2403.18438.

Ji, L., & Peters, A. J. (2003). Assessing vegetation response to drought in the northern Great Plains using vegetation and drought indices. *Remote Sensing of Environment, 87*(1), 85–98.

Justice, C. O., Vermote, E., Townshend, J. R. G., *et al*. (1998). The Moderate Resolution Imaging Spectroradiometer (MODIS): Land remote sensing for global change research. *IEEE Transactions on Geoscience and Remote Sensing, 36*(4), 1228–1249.

Kobayashi, N., Tani, H., Wang, X. & Sonobe, R. (2020). Crop classification using spectral indices derived from Sentinel-2A imagery. *Journal of Information and Telecommunication, 4*(1), 67-90, DOI: 10.1080/24751839.2019.1694765

LeCun, Y., Bengio, Y. & Hinton, G. (2015). Deep learning. *Nature 521*, 436–444. https://doi.org/10.1038/nature14539

Lundberg, S. M., Erion, G. G., Chen, H., *et al*. (2020). From local explanations to global understanding with explainable AI for trees. *Nature Machine Intelligence, 2*, 56–67.

McKee, T. B., Doesken, N. J., & Kleist, J. (1993). The relationship of drought frequency and duration to time scales. Proceedings of the 8th Conference on Applied Climatology (pp. 179–184).

Mehmood, K., Anees, S. A., Rehman, A., Pan, S., Tariq, A., Zubair, M., . . . Luo, M. (2024). Exploring spatiotemporal dynamics of NDVI and climate-driven responses in ecosystems: Insights for sustainable management and climate resilience. *Ecological Informatics*, https://doi.org/10.1016/j.ecoinf.2024.102532.

Muruganantham, P., Wibowo, S., Grandhi, S., Samrat, N.H., Islam, N. (2022). A Systematic Literature Review on Crop Yield Prediction with Deep Learning and Remote Sensing. *Remote Sensing*, *14*, 1990. https://doi.org/ 10.3390/rs14091990

Papagiannopoulou, C., Miralles, D. G., Dorigo, W. A., Verhoest, N. E. C., Depoorter, M., & Waegeman, W. (2017). Vegetation anomalies caused by antecedent precipitation in most of the world. *Environmental Research Letters, 12*(7), 074016.

Prodhan, F. A., Zhang, J., Yao, F., Shi, L., Sharma, T. P., Zhang, D., . . . Mohana, H. P. (2021). Deep Learning for Monitoring Agricultural Drought in South Asia Using Remote Sensing Data. *Remote Sensing, 13*(9), 1715; https://doi.org/10.3390/rs13091715.

Reichstein, M., Camps-Valls, G., Stevens, B., Jung, M., Denzler, J., Carvalhais, N., & Prabhat. (2019). Deep learning and process understanding for data-driven Earth system science. *Nature, 566*(7743), 195–204.

Ribeiro, M. T., Singh, S., & Guestrin, C. (2016). "Why Should I Trust You?" Explaining the Predictions of Any Classifier. KDD 16: Proceedings of the 22nd ACM SIGKDD International Conference on Knowledge Discovery and Data Mining (pp. 1135 - 1144). https://doi.org/10.1145/2939672.29397

Sadiq, M., Sarkar, S. K., & Raisa , S. S. (2023). Meteorological drought assessment in northern Bangladesh: A machine learning-based approach considering remote sensing indices. *Ecological Indicators*, https://doi.org/10.1016/j.ecolind.2023.111233.

Sun, Y., Lao, D., Ruan, Y., Huang, C., & Xin, Q. (2023). A Deep Learning-Based Approach to Predict Large-Scale Dynamics of Normalized Difference Vegetation Index for the Monitoring of Vegetation Activities and Stresses Using Meteorological Data. *Sustainability, 15*, 6632. https://doi.org/10.3390/su15086632.

Tucker, C. J. (1979). Red and photographic infrared linear combinations for monitoring vegetation. *Remote Sensing of Environment, 8*(2), 127–150.

Vasilakos, C., Tsekouras, G. E., & Kavroudakis, D. (2022). LSTM-Based Prediction of Mediterranean Vegetation Dynamics Using NDVI Time-Series Data. *Land, 11*(6), 923; https://doi.org/10.3390/land11060923.

Vicente-Serrano, S. M., Beguería, S., & López-Moreno, J. I. (2010). A multi-scalar drought index sensitive to global warming: The Standardized Precipitation Evapotranspiration Index (SPEI). *Journal of Climate, 23*(7), 1696–1718.

Weiss, J. L., Gutzler, D. S., Coonrod, J. E. A., & Dahm, C. N. (2004). Seasonal and inter-annual relationships between vegetation and climate in central New Mexico, USA. *Journal of Arid Environments, 57*(4), 507–534. https://doi.org/10.1016/S0140-1963(03)00113-7

Willmott, C. J., & Matsuura, K. (2005). Advantages of the mean absolute error (MAE) over the root mean square error (RMSE) in assessing average model performance. *Climate Research, 30*(1), 79–82.

Wu, T., Feng, F., Lin, Q., & Bai, H. (2019). Advanced Method to Capture the Time-Lag Effects between Annual NDVI and Precipitation Variation Using RNN in the Arid and Semi-Arid Grasslands. *Water, 11*, 1789; doi:10.3390/w11091789.

Wu, D., Zhao, X., Liang, S., Zhou, T., Huang, K., Tang, B., & Zhao, W. (2015). Time-lag effects of global vegetation responses to climate change. *Global Change Biology, 21*(9), 3520–3531.

Xiao, X., Ming, W., Luo, X., Yang, L., Li, M., Yang, P., . . . Li, Y. (2024). Leveraging multisource data for accurate agricultural drought monitoring: A hybrid deep learning model . *Agricultural Water Management*, https://doi.org/10.1016/j.agwat. 2024.108692.

Zhang, L., Zhang, L., & Du, B. (2016). Deep learning for remote sensing data: A technical tutorial on the state of the art. *IEEE Geoscience and Remote Sensing Magazine, 4*(2), 22–40. https://doi.org/10.1109/MGRS.2016.2540798

Zhu, X. X., Tuia, D., Mou, L., *et al*. (2017). Deep learning in remote sensing: A comprehensive review and list of resources. *IEEE Geoscience and Remote Sensing Magazine, 5*(4), 8–36.

Zingaro, M., Scicchitano, G., Refice, A., Marsico, A., Kushabaha, A., Elia, M., . . . Capolongo, D. (2024). Assessing the impact of vegetation cover changes and post-fire effects through an enhanced sediment flow connectivity index (SfCI). *Catena*, https://doi.org/10.1016/j.catena.2024.108474.